# Gamma Ray Spectroscopy

Mitchell Kelly* and Noah D'Amico
*University of Florida Department of Physics*
(Dated: April 7, 2023)

A shielded, scintillation crystal and photomultiplier tube apparatus can convert the energy of gamma rays originating from a radioactively decaying source into an equivalent voltage pulse. This pulse can then be processed and sorted using a chain of amplifiers and a multi-channel analyzer into a specific channel where the number of events at that channel can be recorded. The spectrum of this source is produced where specific structures such as photopeaks represent the principal gammas of the decay. It was observed that the high voltage setting limited to 700 V provided the greatest energy resolution, efficiency, and voltage gain. By looking at known gamma energies, a energy calibration curve was produced which had the capability to determine an unknown source's photopeak location within 3.319 keV. Sum peak analysis techniques were utilized to calculate the current activity of a 10 $\mu$Ci $^{22}$Na sodium source with a 4.3 percent error and within the $\pm$10 percent manufacturing specifications of listed activity. Furthermore, The halflife of an excited $^{137}$Ba solution releasing gamma rays was calculated with the Maestro software to be 2.54 $\pm$ 0.00184 minutes.

## 1. INTRODUCTION AND THEORY

Gamma ray photons not originating from cosmic background radiation or other interstellar sources come from the nuclear decay of radioactive (unstable) isotopes. Atoms that are unstable will decay into other progeny (daughter) elements or isotopes, often with the release of ionizing radiation [1]. The rate of nuclear disintegration of the sample is called the activity ($\alpha$), and it is measured in curie, where 1 Ci equals $3.7 \times 10^{10}$ nuclear disintegrations [2]. Radioactive decay via alpha, beta, positron, or electron capture can leave the nucleus in an excited state where the energy released transitioning back to the ground state comes in the form of high energy photons (gamma radiation) [1]. For example, $^{137}$Cs decays into $^{137}$Ba and a $\beta$ particle, and 92 percent of the time the $^{137}$Ba is left in an excited state where a 0.662 MeV gamma is released [2]. Consequentially, we can say that the rate of this gamma's emission is $0.92\alpha$.

If the activity of one source is known than the activity of a different source of the same isotope can be determined by,

$$\alpha_u = \alpha_k \frac{R_u}{R_k} \tag{1}$$

where the count rate is indicated by R, activity by $\alpha$, and subscript labels k and u denoting known and unknown samples respectively.

To measure the energy of a gamma, the energy absorbed into a scintillation crystal is analyzed by the experimental apparatus, discussed further in section 2; however there are several types of gamma interactions which change how much energy can be absorbed into the crystal. A gamma undergoing the photoelectric effect gives up all of its energy to eject a bound inner shell electron from an atom inside the crystal, where the liberated electron's kinetic energy is dissipated by the excitation of other crystal atoms it interacts with [2]. When incident gammas collide with a stationary electron, Compton scattering occurs where

$$E'_\gamma = \frac{E_\gamma}{1 + (E_\gamma/mc^2)(1 - \cos\theta)} \tag{2}$$

Eq. 2 determines the reduction of gamma energy through scattering angle $\theta$. $mc^2$ equals the rest mass energy of the electron, and $E_\gamma$ is the initial energy of the gamma photon [2]. Whenever a gamma Compton scattering off the metal shield enclosing the apparatus deposits all of its energy into the scintillation crystal, its energy is directly calculated by Eq. 2 with $E'_\gamma$ being the energy from some scatter angle $\theta$. More energy is deposited in the crystal when the gamma first Compton scatters inside the crystal and then escapes because the energy absorbed is the kinetic energy of the recoiling electron ($E_e = E_\gamma - E'_\gamma$). Another way in which gamma rays interact is by pair production. Specifically, a gamma ray creates a electron-positron pair ($E_\gamma > 1.022$ MeV) where the pair annihilates contributing the same initial gamma energy as a sum of two 0.511 MeV gammas, yet one or both of these resultant gammas can still escape from the scintillation crystal [2].

## 2. APPARATUS AND EXPERIMENT

The scintillation crystal mentioned previously is a 4×4 inch cylindrical-shaped block of NaI [2]. As seen in Figure 1, the scintillation crystal is attached to a photomultiplier tube (PMT), both encased in a fully reflective covering while the entire apparatus is surrounded by a lead shielding tube [2].

Whenever a gamma ray interacts with the scintillation crystal/PMT apparatus of Figure 1, many photons, called scintillations, are created [2]. To measure and classify what these photons represent, the photons need to be magnified by the PMT, and the photocathode → dynode

*Electronic address: mitchellkelly@ufl.edu

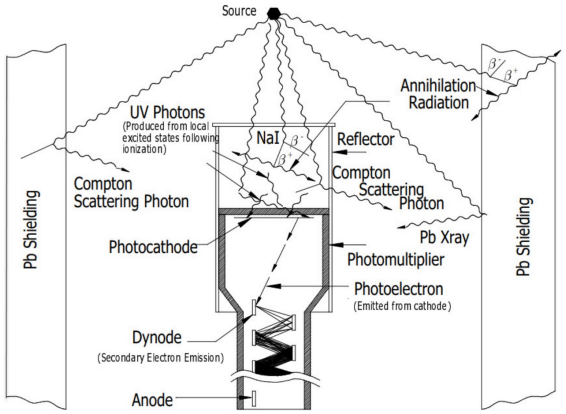


FIG. 1: Schematic diagram of NaI scintillation crystal and surrounding electronics detailed with several types of gamma interactions [3].

→ anode combination accomplishes this task. Scintillations interacting with the photocathode release electrons via the photoelectric effect, and a high voltage (HV) power supply and resistor chain combo transport electrons from the photocathode to the first dynode and so on [2]. Each electron striking a dynode causes 5-10 additional electrons to be liberated into the chain, where at the end, $10^6$ electrons reach the anode [2]. This anode connects to a preamplifier which converts the electrons to an equivalent voltage pulse that is then processed by a linear amplifier [2]. Overall, the apparatus takes the energy of the gamma absorbed in the crustal (amount of scintillations) and proportionally classifies it as a voltage pulse with height representing its magnitude.

The pulse height analyzer (PHA) takes in linearly amplified voltage pulses, determines the maximum pulse height, and sorts it into channels based upon said maximum. This PHA analyzes pulse heights ranging from 0-10 V while being sorted into 1024 channels [2]. The complimentary Maestro PHA software plots these channel numbers with the counts in each channel to create a graph representing the nuclear composition of the radioactive source. A photopeak is observed when all the energy of a gamma is deposited into the scintillator, and Figure 2 shows what photopeaks look like in the spectrum.

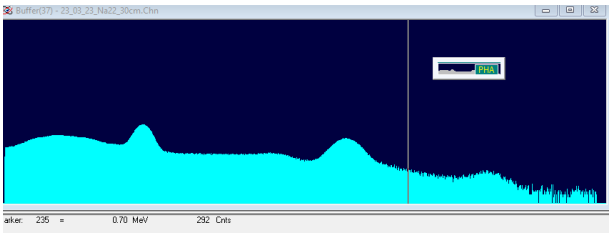


FIG. 2: Maestro PHA software detector counts (vertical axis) versus channel number (horizontal axis) from a sodium source possessing two photopeaks in its spectrum.

Additionally, note that statistical fluctuations in measurement cause a 5-10 percent width in the peak, so a Gaussian-looking structure is depicted as the entire resultant peak [2]. Backscatter and Compton edge peaks occur whenever gammas Compton scatter into the crystal off of the lead shielding with reduced energy or if a gamma Compton scatters inside the crystal, respectively. Gammas can hit the detection system at a rate that the program cannot process, so the Maestro program corrects for this "dead time" with a "live time" that actually represents when measurements were not busy being processed by the program. The amount of dead time is proportional to the amount of gamma events interacting with the scintillator, so the closer a source is to the crystal, the greater the percentage of dead time.

$$E_\gamma = \kappa C_\gamma + E_0 \tag{3}$$

An energy calibration utilizing Eq. 3 was conducted, where $\kappa$ represents the energy scale (energy/channel), $C_\gamma$ equals the channel number, and $E_0$ being the energy offset [2]. Measurements of the photopeak positions for well-known sources ($^{137}$Cs, $^{22}$Na, $^{60}$Co, and $^{152}$Eu) were used and fitted to Eq. 3 via linear regression. All sources were situated around 20 cm away from the detector front edge to minimize effect of photopeak position being lowered at high count rates. The calibration curve was then used to estimate the photopeak energy of an unknown radioactive substance, and a background radiation subtraction was employed to ensure the photopeak came from the unknown source itself.

Moreover, the efficiency, gain, and energy resolution's dependence on the PMT's high voltage setting was analyzed with a $^{137}$Cs spectrum at the 700, 800, and 900 Voltage levels (Distance from source held constant). The width of a photopeak, measure of energy resolution of the apparatus detection system, is given by

$$R = \frac{\Delta C}{C} \tag{4}$$

where $C$ is the channel number and $\Delta C$ is the full width at half maximum (FWHM) of the peak [2]. How small the width the system can measure, equates to how close two gamma ray energy photopeaks can still be seen as separate distinct peaks, which comes into play for sources such as $^{152}$Eu with 10 different principal gammas.

Activity measurements of 10 $\mu$Ci $^{22}$Na 10-30cm away from the detector were compared to the expected activity of the sample at the time of experiment. With the addition of sum peak analysis techniques, the activity is given by

$$\alpha = \frac{1}{t_l}\left(C_t + \frac{C_1 C_2}{C_{12}}\right) \tag{5}$$

where $t_l$ is the live time, and $C_1, C_2, C_{12}$ represents the total counts in photopeaks 1 and 2, and the sum peak (12). The small photopeak rightwards of the center peak

in Figure 2, represents a sum peak, a photopeak corresponding to two gammas simultaneously detected by the Maestro program [2]. This photopeak resides in the channel corresponding to the energy summation of both gammas [2].

Since nuclear decay is a homogeneous Poisson process, the halflife of excited $^{137}$Ba can be estimated through nonlinear regression with a probability distribution of $dP = \Gamma e^{-\Gamma t} dt$ and halflife $\tau \ln(2)$ [2]. Powdered $^{137}$Cs was mixed with a mild acid to cause beta emission where $^{137}$Ba was the resultant product of decay; however, this excited $^{137}$Ba decays to its ground state with a half life in the range of minutes, releasing a gamma [2]. The barium was collected into a dish up against the detector for 1600 seconds to acquire enough data for the halflife measurement and associated uncertainty.

## 3. ANALYSIS AND RESULTS

Eq. 4 was used to evaluate the resolution for 700, 800, and 900 V in the high voltage dependence study where the results were as follows: 0.084 for 700 V, 0.076 for 800 V, and 0.074 for 900 V. Additionally, it was observed that the photopeak center channel at 700, 800, 900 V was 595.6, 592.6, and 586.5 respectively. Thus, it can be concluded that the 700 V setting yielded the greatest resolution and voltage gain alike. The resolution was more sensitive with respect to the voltage around 700 V, but not as much for 800 and 900 V. The increase in voltage did not change the photopeak count rate, but at lower voltages a higher entire spectrum count rate was observed. If higher voltages are necessary in the spectrum photopeak measurement, it is more beneficial to not exceed 700 since the resolution and gain are maximized.

| **Distance** (cm) | $\boldsymbol{\alpha}$ (Ci) | $\boldsymbol{\sigma_\alpha}$ (Ci) |
|---|---|---|
| 1.5 | 282451.3 | 1843.3 |
| 5 | 250998.2 | 3914.5 |
| 11 | 240314.0 | 7680.0 |
| 20 | 239707.1 | 14861.2 |
| 25 | 251776.0 | 24678.8 |
| 30 | 348002.1 | 34043.8 |

TABLE I: 10 $\mu$Ci $^{22}$Na activity measurements and their uncertainty over several distances away from detector.

Table I's calculations were created utilizing Eq. 5 with consideration of a dead time correction ($R_m = \frac{R}{1+RT}$) with $R$ equal to the true count rate, $R_m$ representing the measured count rate, and $T$ as the dead time associated with each measurement. Converting the average value of the activities into Ci, the current activity of the 10 $\mu$Ci $^{22}$Na source was 7.27 $\mu$Ci. The sample was created approximately 3/4 of a year ago with a likely activity of 9.57 $\mu$Ci at the time of conception. Considering that manufacturer activities have a $\pm$10 percent uncertainty, the calculated expectation based upon the data of Table I falls within this accepted region.

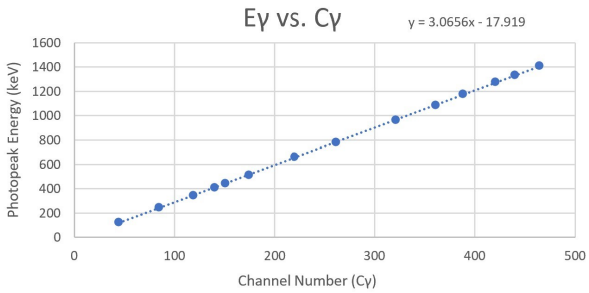


FIG. 3: Energy calibration graph of $^{137}$Cs, $^{22}$Na, $^{60}$Co, and $^{152}$Eu principle photopeak energies versus the recorded channel number.

Figure 3 illustrates the linear relationship, defined by Eq. 3, between the calibration sources' gamma energy and photopeak center channel number of that gamma. A linear regression program was utilized to determine the correlation between the variables and define a line of best fit. Its equation, $E_\gamma = 3.0656 C_\gamma - 17.919$, and graphical representation of a trend line is observed in Figure 3. The standard error ($\sigma_{E_\gamma}$) was determined to be 3.319 keV via the program, so the unknown sample's true photopeak energy lied between plus and minus this uncertainty at the following measurement. The unknown sample's channel number was observed to be 483.9, so its calibrated photopeak energy was calculated at 1462.4 $\pm$ 3.319 keV. According to LD-Didactic, $^{40}$K undergoes a $\beta^+$ decay into $^{40}$Ar where a gamma of energy 1460.81 keV is emitted [4]. Analyzing the sample's physical characteristics, shelf life in the order of magnitude of decades, and proximity to the accepted gamma ray energy of $^{40}$K decay, the unknown sample was confirmed to be Potassium salt (KCl), which contains trace elements of $^{40}$K.

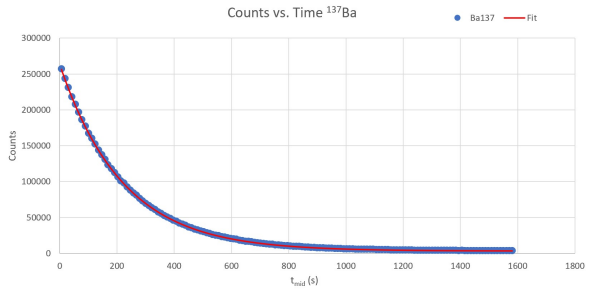


FIG. 4: Excited state $^{137}$Ba decay gamma count data versus time with inclusion of nonlinear fit.

As seen in Figure 4, the count rate of gammas coming from $^{137}$Ba transitioning to its ground state was an exponential probability distribution, and its nonlinear re-

gression was facilitated by

$$C_p = C_B + C_0 e^{-t_{mid}/\tau} \tag{6}$$

where $C_B = R_B t_l$, $C_0 = R_0 t_l$, and $\tau$ equals the mean lifetime of the $^{137}$Ba excited state. Additionally note that subscripts $B$ and 0 associated with $R$ represent background count rates and event count rates while $t_l$ and $t_{mid}$ indicate live time and time bewteen measurement. Minimization of the $\chi^2$ with respect to the fitting parameters of Eq. 6 was conducted to find the best graphical fit and values of the fitting parameters. $\tau$ in Eq. 6 was calculated to be 219.7 seconds. Its uncertainty was calculated through the square-root of its corresponding diagonal element in the parameter covariance matrix, and that uncertainty was 0.146 seconds. Thus, the halflife of $^{137}$Ba was calculated to be 2.54 $\pm$ 0.00184 minutes.

## 4. CONCLUSIONS

The analysis of the high voltage dependence on efficiency, gain, and resolution led to the conclusion that compared to the 800 and 900 V settings, 700 V maximized all categories. Conducting this investigation several more times with more high voltage settings could help pinpoint better voltage settings for the categories while eliminating random error associated with fluctuating count rates. Although the activity measurements of 10 $\mu$C $^{22}$Na revealed that the calculated original activity had a 4.3 percent error compared to the manufacturer specified value, the experiment could be improved to yield more accurate results. The solid angle between the detector and sample was not considered which could change activity values when the distance between them got increasingly large. Additional studies on $^{22}$Na sources of varying activity can be pursed for more analysis as well.

Most sources of systematic error for the experiment come from the apparatus determining an accurate voltage pulse for a given gamma. The Maestro program had a built-in dead time correction installed to account for this increasing the chance of systematic error, yet the programming of all the components cannot eliminate it entirely. Random error played a role in the halflife measurement of excited $^{137}$Ba because the percent error between the observed and true halflife was 0.39 percent even though the measurement did not fall within the one sigma range of the accepted value. An extremely accurate measurement was recorded, but this measurement was too far off. Conducting additional trials of the halflife experiment should eliminate most of the random errors associated with it. The energy calibration curve was accurate enough to determine an unknown isotope of a radioactive substance with an error of 3.319 keV that was within the bounds of the photopeak channel number uncertainty. A quadratic term could be added to account for any slight deviations, yet it was not necessary to reduce the systematic error of the measurement device.


[1] S. Keith, *Toxicological Profile for Radon* (2012), URL https://www.ncbi.nlm.nih.gov/books/NBK158792/.

[2] R. DeSerio, *Gamma ray spectroscopy*, https://www.phys.ufl.edu/courses/phy4803L/group_I/gamma_spec/gamspec.pdf (2023), Phy 4803L, Department of Physics, University of Florida.

[3] J. L. Duggan, *Laboratory Investigations in Nuclear Science* (The Nucleus, 1988).

[4] L. Didactic, *Potassium-40*, URL https://www.ld-didactic.de/software/524221en/Content/Appendix/K40.htm.